2010 IEEE International Conference on Robotics and Automation
Anchorage Convention District
May 3-8, 2010, Anchorage, Alaska, USA

Performance Study of a Fish Robot Propelled by a Flexible Caudal Fin

K. H. Low, C. W. Chong, and Chunlin Zhou

***Abstract* — In this paper, a fish robot employing a carangiform swimming mode is adopted as an experimental platform for the parametric study. Experiments conducted in the laboratory aim to study the variation of robotic fish's thrust with respect to various parameters including the frequency and amplitude of oscillation, joint link, aspect ratio, free flow velocity and the spring effect. The testing also enables us to find out the relationship between various parameters and the thrust generated by the oscillatory motion of tail. On the other hand, the significance of the controlled parameters will be determined using statistical methods.**

I. Introduction

THE robotics engineering community has long been impressed with the swimming speed and agility of fish. They have been focusing on developing a new technique of propulsion by mimicking the nature. Biorobotic technology has become one of the hotspots in underwater robotics research in recent years [1]. A biomimetic robot is the combination of fish-like propulsive mechanism and robotics technology. The purpose of this research is to investigate the feasibility of an oscillating propulsion system for underwater vehicles. An oscillating fin propulsion system with one actuated joint and two passive joints (including the spring joint) has been developed, which is much simpler as compare the other robotic fishes developed by other researcher (many of which have multi-link driven by multiple motors) [2-9]. The two passive joints reduce the numbers of motors required at each link; hence reduce the total moment of inertial of the oscillating fin propulsion system, but yet, able to mimic a carangiform swimming motion. Experiments were carried out to determine the effects of various parameters on the thrust and velocity of the robotic fish. Lastly, conclusion about the performance of the system and future enhancement will be presented.

The robotic fish (NAF-I) proposed in this study mimics the fish, mostly from carangiform to ostraciiform, where the undulations generated through the last three segments of the body muscle mass [10] (Fig. 1). These swimmers are generally faster than anguilliform or subcarangiform swimmers [11]. The design of the robot and the water tunnel experimental setup will be presented first. Thereafter, a statistical analysis on the significance effect of various parameters on the output thrust generated will be discussed [11].

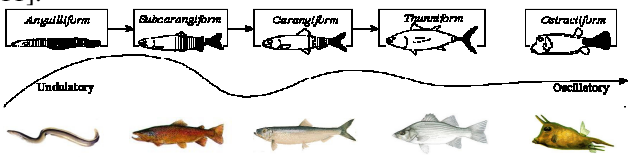

Fig. 1. BCF Swimming Modes [12]

II. Design of Fish Robot

To mimic the fish propulsion mainly by tail, we have developed a robotic fish, Nanyang Awana (NAF-I) [11], whose CAD model is shown in Fig. 2. The NAF-I comprises of four individual modules: tail fin module, electronics housing module, ballast tank module, and fish head module (including control and power units [13]). As they are designed in a modular manner, the modules can be easily replaced should there be a change in the design or additional functions are required to be incorporated to the robotic fish.

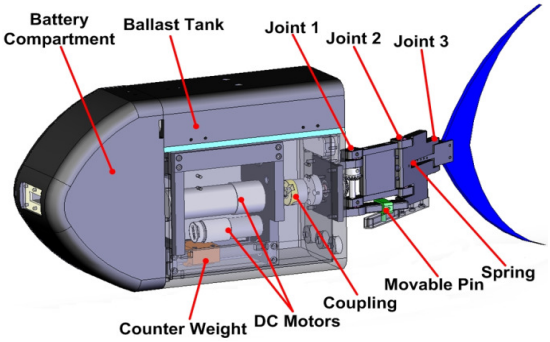

Fig. 2. CAD model of robotic fish designed, Nanyang Awana (NAF-I) [11]

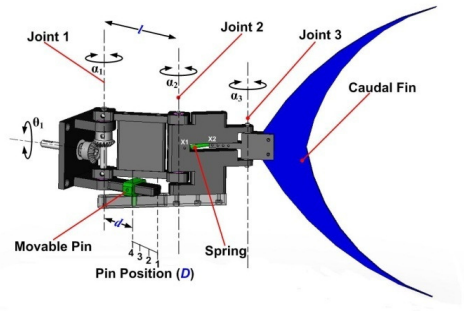

Fig. 3. CAD Model of Caudal Tail Fin Module.

Revised manuscript received on February 2, 2010. This work is supported in part by the MoE AcRF Research Grant RG23/06.

K. H. Low is professor with the School of Mechanical and Aerospace Engineering, Nanyang Technological University, Singapore 639798; e-mail: mkhlow@ntu.edu.sg.

C. W. Chong and Chunlin Zhou are research students with the School of Mechanical and Aerospace Engineering, Nanyang Technological University, Singapore 639798.

The main propulsion method employed in NAF-I is the use of the caudal tail fin (Fig. 3) – a common swimming gait used by carangiform swimmers, such as the arowana or the herring. The relevant specifications of the NAF-I are tabulated in Table I.

TABLE I
SPECIFICATION OF NAF-I [11]

Symbol	Quantity
Mass	Approximate 6.8 kg
Dimension	661mm (L) x 260mm (H) x 100mm (W)
Actuator	2 units of Maxon RE25 DC Micromotor
Microcontroller	Microchip PIC18F-2431
Power source	15VDC, 4000mAH Ni-H battery
Swimming speed	0.33 m/s, ½ BL/s (max)
Swimming mode	Straight, turning, diving and surfacing
Turning radius	0.1 m
Operating time	Approximately 4 hours (fully charged)
Communication	FM radio frequency

I. EXPERIMENTAL SETUP & PROCEDURE

A. *Design of Experiment (DOE)*

A set of experiments is designed to evaluate the performance of NAF-I. Six controllable parameters can be covered in the experiments: frequency (f), amplitude (θ_1), movable pin position (D), aspect ratio (r), spring constant (k) and water tunnel flow velocity (v). Those parameters are selected based on several principles: 1) they are thought to be significant in related research fields especially in flapping foil and biological areas; 2) suitable for the experiment methodology; and 3) closely related to the design of the robot. The levels for each parameter are also selected based on the literature review, design of the robot and limitations of experiment equipments. When selecting the levels for those parameters, the prototype capability, force transducer limitation and the range of practical application were considered. For example, three spring constants (k) were considered in this experiment, although more can be provided. The levels with the ranges of the six parameters selected are given in Table II.

TABLE II
LEVEL FOR THE INPUT PARAMETERS

Lever Parameters	1	2	3	4	5	6
Frequency, f (Hz)	0.4	0.8	1.2	1.6	2.0	2.4
Amplitude, θ_1 (deg)	6	8	10	12	14	16
Pin position, D (mm)	0	5	10	15		
Aspect ratio, r	8.71	6.82	4.80	3.21		
Spring, k (N/mm)	0.98	2.45	4.61			
Flow velocity, v (m/s)	0.034	0.102	0.171			

There would be a total of 5184 runs, if all ranges of control parameters and levels would all be considered in the experiments. To reduce the consumed time in achieving the results, various strategies can be adopted for an appropriate choice of runs. One of the strategies is the Taguchi's orthogonal scheme [14]. The design of the experiments includes two sets of testing steps. Firstly, for Set one, six process parameters; frequency (f), amplitude (θ_1), Movable pin position (D), aspect ratio (r), spring constant (k), and water tunnel flow velocity (v) were designed by a six-factor and mixed-level orthogonal scheme, which required 49 runs. A further 120 tests were then considered to provide sufficient "as measured" data for statistical analysis.

B. *Experimental Setup*

The experiment was conducted in the water tunnel system equipped with a water pump (which can provide maximum speed of 0.17 m/s linear velocity at the test section), a high transparency tempered glass test section, electronic flow control panel, and an array of screeners to provide the laminar flow (Fig. 4). Fig. 5 shows the actual setup of the robotic fish prototype in the water tunnel's test section and the axis of arrangement for the force transducer. An ATI-Gamma six-axis force transducer was used for recording the thrust force produced by the robotic fish. The transducer reacts to the applied forces and torques from the experiment.

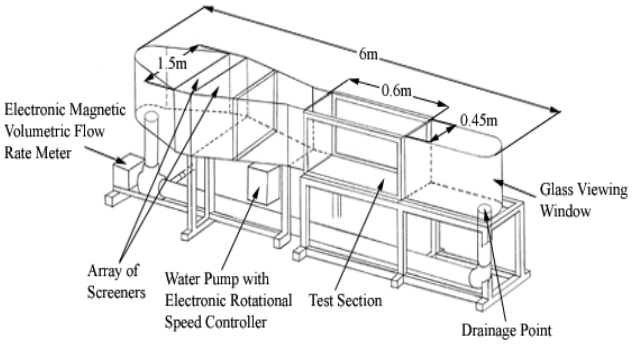

Fig. 4. General layout of water tunnel system [15].

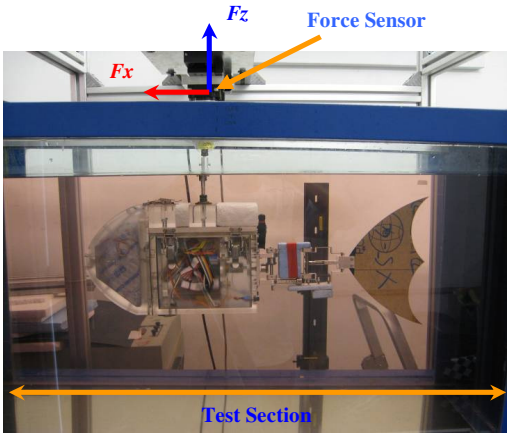

Fig 5. NAF-I mounted in the Test Section of water tunnel system [11]

In order to quantitatively evaluate experimental results, a measurement of the force along with the direction of the water flow was made. After the flow in the water tunnel become stable, the force sensor value was bias to zero, thereafter; the robotic fish was turned on. With water flow rates and with tail motion, the x-force transducer will measure the net force of the thrust produced by the tail and the drag forces induced by the tail motion and the body drag force as shown by:

$$F_x = F_{x-system} = F_t - F_d \quad (1)$$

where F_d is the body drag and F_t is the net thrust generated by the tail. The force generated in the 30 oscillation cycles after the first five cycles were recorded by the force transducer. The average value of the recorded data was considered as the reference measurement of the test run. Three measurements were taken each test run and the average of the three was used as the final reading.

II. Results

A. Analysis of Variances (ANOVA)

In order to identify the parameters that are significant in affecting the output thrust of the fish robot, an ANOVA has been carried out. Fig. 6 (a-f) show the trends of each individual parameter plotted, using the data from the 169 runs of test as discussed earlier. We can notice that all the controlled parameters within the tested range/levels can be considered having a linear relationship with the output force generated. Hence, a simple general linear model Analysis of Variance (ANOVA) test can be used to determine how significant of each controlled parameter has on the output force. The result of the ANOVA is tabulated in Table III.

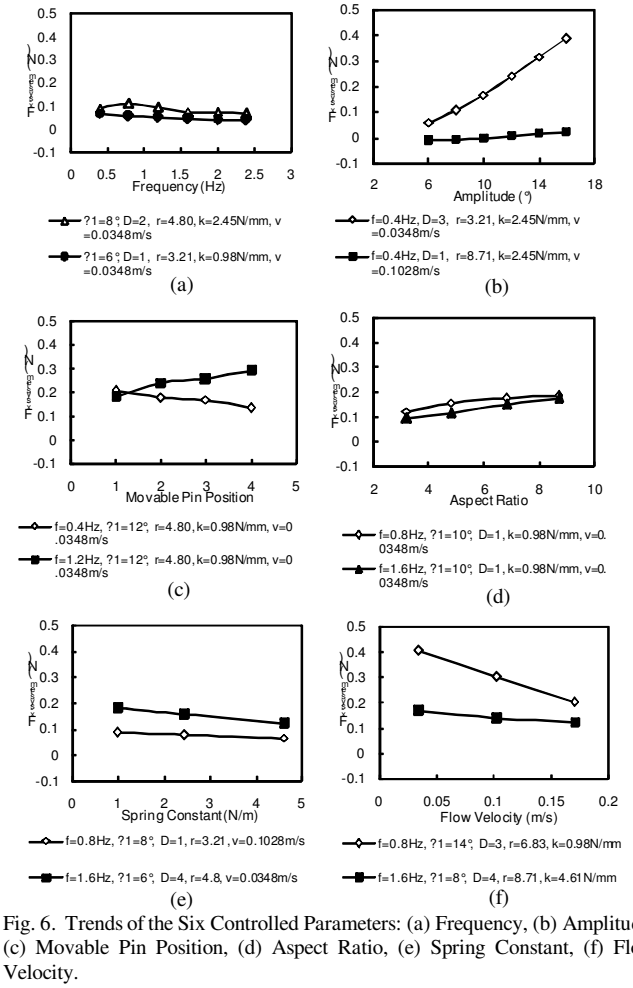

Fig. 6. Trends of the Six Controlled Parameters: (a) Frequency, (b) Amplitude, (c) Movable Pin Position, (d) Aspect Ratio, (e) Spring Constant, (f) Flow Velocity.

It shows in Table III that the main effect θ_1 and v have significant effect on the output thrust, since both of them have a value of 0.000 (<0.05). Besides, the interaction between the frequency and the movable pin position (f*D) also have a significant effect on the output thrust. Hence, with f*D having significant effect on the output thrust, we cannot exclude factor f and D from further testing although their main effect does not have significant effect on the output thrust.

TABLE III
ANOVA of the Six Controlled Parameters
Dependent Variable: Thrust

Source	F	Sig. <0.05
f	3.409	.053
θ_1	34.099	.000
D	1.427	.298
r	1.489	.282
k	1.675	.241
v	69.344	.000
f * θ_1	.190	.959
f * D	8.062	.006
f * r	1.665	.241
θ_1 * D	.839	.506

R Squared = .998 (Adjusted R Squared = .976)

It is noted that the 49 runs generated from the orthogonal design are only sufficient to calculate the significances for the main effect (f, θ_1, D, r, k, v). The additional 60 runs of test actually allow the software to solve for several second order interaction (f*D, f*θ_1, etc.), but not all. But this will not affect the result of the interpretation from the ANOVA table. We can assume that the other 2nd and higher order interaction will not have significant effect on the output thrust except the interaction f*D which were found to have significant effect on the output thrust. According to the ANOVA results, the aspect ratio (r) and the spring constant (k) were found to have no significant effect on the output thrust. However, we would like to take a closer look on how the aspect ratio and the spring constant influence the output thrust since, studies [16-18] have shown that both aspect ratio and spring flexibility had influence on the output thrust.

B. Effect of Aspect Ratio

It can be seen from Figs. 7a and b that a higher aspect ratio actually performed better as compared to the lower one. Nevertheless, one has to take note that for this experiment setup; the area of the smallest aspect ratio tail fin is made larger than that of the higher aspect ratio tail fin (refer to Fig. 8). Thus, we would have expected more forces to be generated by a larger fin, but the results did not support that. Hence, we would say that a larger thrust force could be generated by using a higher aspect ratio tail fin, but not the one with small aspect ratio and larger tail fin area. Thus, in the future studies, the highest aspect ratio (8.71) will be used for optimum performance.

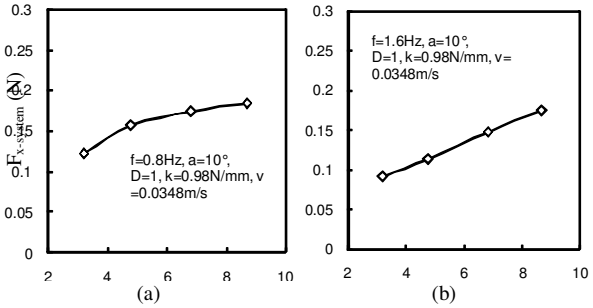

Fig. 7. Effect of the Aspect Ratio (r) on the Output Thrust.

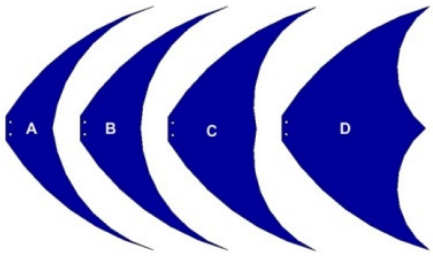

Fig. 8. Type of Tail Fins Tested: Area A: 7711 mm^2, Aspect Ratio: 8.71; Area B: 9906 mm^2, Aspect Ratio: 6.82; Area C: 14096 mm^2, Aspect Ratio: 4.80; Area D: 21082 mm^2, Aspect Ratio: 3.21.

C. *Effect of Spring Constant*

The result in ANOVA discussed earlier shows that the spring constant does not have a significant effect on the output thrust generated by the oscillating fin, which is possibly caused by the inadequate range of spring constant used in the experiment. An additional experiment was carried out by constraining the spring joint (joint3 - refer to Fig. 3), which can now be modeled as a rigid joint with very high spring constant value, in turn, making the range of the spring constant wider. From Fig. 9, it can be seen that the output thrust generated with a flexible joint (low spring constant of 0.98N/mm and 2.45 N/mm) is much higher than the one with a rigid joint (high spring constant) and the effect of the spring constant is more obvious when the sweeping amplitude is larger than 10 degree. This increase in the net thrust force for a flexible tail joint is most likely due to the drag reduction on the tail fin. One can also noticed that the values of the thrust between spring constant of 0.98 N/mm and 2.45 N/mm are very close to one another. This result have supported our hypothesis that previous selected spring constant range for the ANOVA analysis was indeed too narrow to shows the significance of the spring effect.

From this analysis, a flexible joint is much more preferred if a larger output thrust force is desired. This result also indicates a certain degree of drag reduction with this form of propulsion method by using a low spring constant. Thus, for the detailed studies on the effect of the oscillating frequency (f) and amplitude (θ_1), the value of the aspect ratio (r) and spring constant (k) are kept at their optimal values (8.71 and 0.98 N/mm respectively).

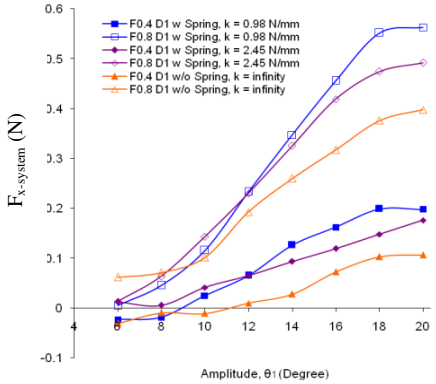

Fig. 9. Effect of Spring Constant on the Output Thrust with v = 0.0348 m/s and r = 8.71.

D. *Effect of Frequency*

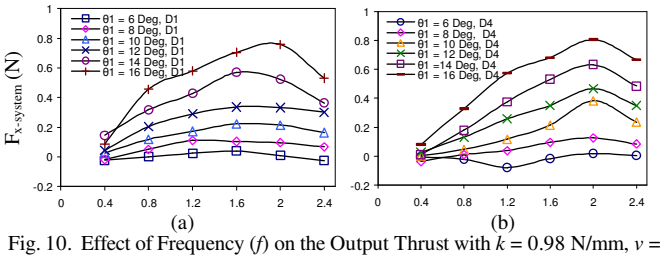

Fig. 10. Effect of Frequency (f) on the Output Thrust with k = 0.98 N/mm, v = 0.0348 m/s and r = 8.71.

Fig. 10 (a) and 10 (b) shows the effect of frequency on the output thrust at movable pin position '1' (D1) and '4' (D4) respectively. It can be noticed that the output thrust increases as the frequency increases and it peaks at a frequency of around 2 Hz for most of the runs. Thereafter, the output thrust decreases with a further increase in frequency. The peak at 2 Hz was originally thought to have caused by the speed limitation of the motor when operating at a high frequency, but the experiment result shows that it is not the case. Another possibility of the peak might be due to the natural frequency of the system. We also find that the non-linearity between the oscillating f and the D on the output thrust of the oscillating fin (see Fig. 11). From the experiments result, it is noticed that movable pin position 'D1' generates larger output thrust as compared to 'D4' when operated at a frequency of 1.6Hz and below. When the operating frequency is above 1.6 Hz, movable pin position 'D4' will be more preferred as it generates a higher output thrust.

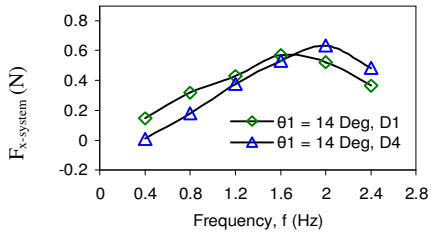

Fig. 11. Interaction between the Frequency and the Movable Pin Position on the Output Thrust

E. Effect of Amplitude

Figs. 12 (a-d) show the effect of the amplitude (θ_1) on the output thrust. Learning from previous experiments done by other researcher [16, 19], one would have expected to see an increasing trend up to a peak point and then followed by a decreasing trend. The increasing trends are shown very clearly in Figs. 12 (a-d), but not for the peak and decreasing trend.

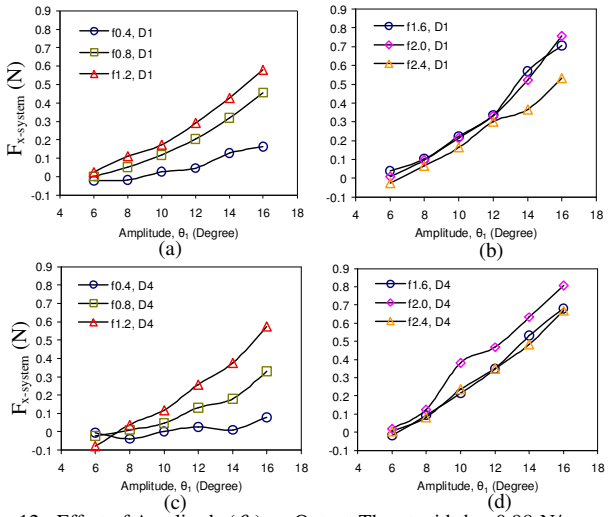

Fig. 12. Effect of Amplitude (θ_1) on Output Thrust with k = 0.98 N/mm, v = 0.0348 m/s and r = 8.71.

Due to the mechanical linkages of the tail fin design, it may not be adequate to just looked at the effect of the amplitude (θ_1) on the output thrust, since the tail end position is depended not only on the amplitude (θ_1) alone, but also the movable pin position (D). Hence, in order to have a clearer understanding on why the peak occurred at these ranges, we will like to look at the effect of the sweeping amplitude (Q, see Fig. 13) on the output thrust. As studies have shown that, the (double) sweeping amplitude to fish length ratio for all species of fish was in a range of 0.20 to 0.24. For high propulsion efficiency, the sweeping amplitude of the fish should be around 10 to 12 percent of its body length [17]. Hence, we would like to determine whether the peak we observed earlier lies within this range.

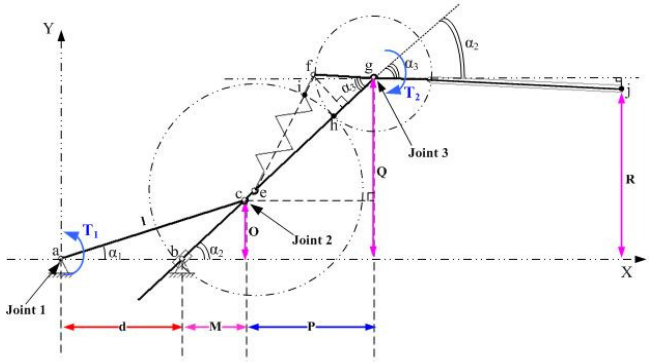

Fig. 13. Kinematics Diagram of the Caudal Tail Fin Mechanism [11].

The value of the sweeping amplitude (Q) for each corresponding amplitude (θ_1) and movable pin position (D) can be found by:

$$Q = l\sin\alpha_1 + cg\left[\sin\left(\tan^{-1}[(l\sin\alpha_1)/(l\cos\alpha_1 - d)]\right)\right] \quad (2)$$

where l is the distance from point 'a' to point 'c' and cg is the distance from point 'c' to point 'g'. The values of sweeping amplitude (Q) and the percentage ratio of it to the fish's length were tabulated as shown in Table IV.

TABLE IV
UNITS FOR MAGNETIC PROPERTIES VALUE OF SWEEPING AMPLITUDE (Q) AND PERCENTAGE OF SWEEPING AMPLITUDE TO FISH'S LENGTH RATIO FOR EACH CORRESPONDING VALUE OF AMPLITUDE (θ_1).

Amplitude θ_1, degree	**Sweeping Amplitude Q, mm (D1)**	**Percentage of Q to Fish's Length Ratio, %**	**Sweeping Amplitude Q, mm (D4)**	**Percentage of Q to Fish's Length Ratio, %**
6	34.9	5.28	22.43	3.39
8	44.62	6.75	29.63	4.48
10	53.18	8.05	36.61	5.54
12	60.65	9.18	43.34	6.56
14	67.15	10.16	49.78	7.53
16	72.83	11.02	55.92	8.46
18	77.83	11.77	61.75	9.34
20	82.27	12.45	67.26	10.18
22	86.24	13.05	72.47	10.96
24	89.83	13.59	77.36	11.7

With the values found in Table IV, the output thrust against the percentage of sweeping amplitude to fish's length ratio were plotted and were shown in Figs. 14 (a & b). It can be seen that the peak indeed occurs in the range (10 to 12 %) observed by other researcher. Although the decreasing trends were not fully observed, but from the slopes of the trend, it seems highly that the peak would lie in the optimal range of 10 to 12 percents. Hence, it can be concluded that to obtain a maximum thrust force, the sweeping amplitude (Q) should be kept within the range of 10 to 12 percent of the fish's body length.

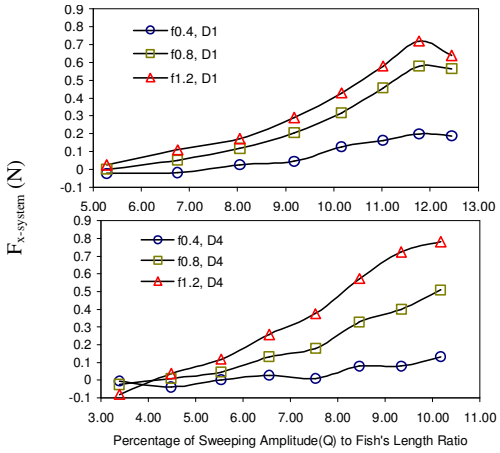

Fig. 14. Effect of the Percentage of Sweeping Amplitude to Fish's Length Ratio on the Output Thrust at D1 (upper) and D4 (lower), where k = 0.98 N/mm, v = 0.0348 m/s, and r = 8.71.

For the relationship between the oscillating frequency and amplitude, under a constant oscillating velocity, the run with a lower frequency and higher amplitude always generates a larger thrust as compared to the one with higher frequency

and lower amplitude. This result implied that, if we required a higher thrust (normally during accelerating or moving from rest), it will be better to operate the tail fin at a lower frequency and a high amplitude. Once it reached a constant speed, a low-amplitude and high-frequency setting is preferred.

III. Concluding Remarks

Parametric studies on the fish-like underwater vehicle were conducted in the water tunnel system to determine the effect of the various parameters on the output thrust generated by the oscillating fin. The result from the statistic test had shown that the parameter frequency (f) and amplitude (θ_1) have significant effects on the output thrust. Although the spring constant was not found to have significant effect on the output thrust, a further experiment testing have shown that the inadequate range of spring constant used in the studies may cause its insignificance. The experimental studies on the effect of the flexible passive spring joint have shown the signs on drag reduction. From the experiment analysis, we have found that in order to produce a larger thrust force, the selection of the parameters plays a very important part. From the studies, a combination of a relatively high frequency (2.0 Hz), a sweeping amplitude (Q) to fish's length ratio of about 0.1-0.12, a high aspect ratio (8.71), a movable pin position at 'D4'and a softer spring (0.98 N/mm) can produce the largest thrust force.

This work provides a guideline for the selection of various parameters to increase the swimming performance of the fish robot. However, in order to effectively control and optimize the output thrust and swimming speed of the fish robot on a mathematical and quantitative basis, it is essential to develop predictive models, in future, for the thrust generation and swimming velocity of the fish robot. The model formulated is believed to be useful in future navigation control of the fish robot. This model can also be used as a guideline for others to develop their fish robot's mechanism based on the predictive thrust and swimming speed required.

Acknowledgment

The authors would like to thank Professor John Davenport, University College Cork, Ireland, and Professor Srigrarom Sutthiphong of the NTU for sharing their knowledge and providing the resources for conducting the experiments.

References

[1] R. L. Wernli, "AUVs-the maturity of the technology," Seattle, WA, USA, pp. 189-95, 1999.

[2] N. Kato, "Control performance in the horizontal plane of a fish robot with mechanical pectoral fins," *IEEE Journal of Oceanic Engineering,* vol. 25, pp. 121-129, 2000.

[3] S. Saimek and P. Y. Li, "Motion planning and control of a swimming machine," *International Journal of Robotics Research,* vol. 23, pp. 27-53, 2004.

[4] M. A. MacIver, E. Fontaine, and J. W. Burdick, "Designing future underwater vehicles: Principles and mechanisms of the weakly electric fish," *IEEE Journal of Oceanic Engineering,* vol. 29, pp. 651-659, 2004.

[5] N. E. Leonard, "Control synthesis and adaptation for an underactuated autonomous underwater vehicle," *IEEE Journal of Oceanic Engineering,* vol. 20, pp. 211-220, 1995.

[6] P. Y. Li and S. Saimek, "Modeling and estimation of hydrodynamic potentials," in *Proceedings of the IEEE Conference on Decision and Control*, Phoenix, Arizona, USA, pp. 3253-3258, 1999.

[7] K. H. Low and A. Willy, "Biomimetic motion planning of an undulating robotic fish fin," *JVC/Journal of Vibration and Control,* vol. 12, pp. 1337-1359, 2006.

[8] P. T. Madsen and R. Payne, "How Ships' Traffic Noise Affects Whales in a Shipping Channel," 2003.

[9] K. H. Low, C. Zhou, and Y. Zhong, "Gait planning for steady swimming control of biomimetic fish robots," *Advanced Robotics,* vol. 23, pp. 805-829, 2009.

[10] C. M. Breder, "The locomotion of fishes," *Zoologica,* vol. 4, pp. 159-297, 1926.

[11] C. W. Chong, Y. Zhong, C. L. Zhou, K. H. Low, and G. Seet, "Can the swimming thrust of BCF biomimetics fish be enhanced?," *Proc. IEEE Int. Conf. on Robotics and Biomimetics,* pp. 437-442, 2009.

[12] C. C. Lindsey, *Form, function and locomotory habits in fish* vol. VII Locomotion. New York: Academic Press, 1978.

[13] C. L. Zhou, C. W. Chong, Y. Zhong, and K. H. Low, "Robust gait control for steady swimming of a carangiform fish robot," in *IEEE/ASME International Conference on Advanced Intelligent Mechatronics (AIM)*, Singapore, 2009.

[14] Y. Y. G. Taguchi, Y. Wu, *Taguchi Methods: Design of Experiments*: American Supplier Institute, 1993.

[15] W. M. Tan, W. S. V. Chai, and S. Srigrarom, "Kinetics of pitching SD8020, CH10SM, M06-13-128, and NACA 2414 hydrofoils," *Journal of Flow Visualization and Image Processing,* vol. 15, pp. 329-336, 2008.

[16] P. Prempraneerach, F. S. Hover, and M. S. Triantafyllou, ""The effect of chordwise flexibility on the thrust efficiency of a flapping foil"," *13th Int. Symp. Unmanned Untethered Submersible Techn.,* 2003.

[17] G. S. Triantafyllou, M. S. Triantafyllou, and M. A. Grosenbaugh, "Optimal Thrust Development in Oscillating Foils with Application to Fish Propulsion," *Journal of Fluids and Structures,* vol. 7, pp. 205-224, 1993.

[18] M. Sfakiotakis, D. M. Lane, and J. B. C. Davies, "Review of fish swimming modes for aquatic locomotion," *IEEE Journal of Oceanic Engineering,* vol. 24, pp. 237-252, 1999.

[19] J. J. Magnuson, "Locomotion by scombrid fishes: Hydromechanics, morphology and behavior," *Fish Physiology,* vol. 7, pp. 239-313, 1978.